Available online at www.sciencedirect.com

SciVerse ScienceDirect

journal homepage: www.elsevier.com/locate/he

Transport properties and fuel cell performance of sulfonated poly(imide) proton exchange membranes

Jingling Yan [a], *Xiaoming Huang* [a], *Hunter D. Moore* [a], *Chao-Yang Wang* [a,b], *Michael A. Hickner* [a,*]

[a] *Department of Materials Science and Engineering, The Pennsylvania State University, University Park, PA 16802, USA*
[b] *Department of Mechanical Engineering, The Pennsylvania State University, University Park, PA 16802, USA*

ARTICLE INFO

Article history:
Received 7 March 2011
Received in revised form
18 September 2011
Accepted 20 September 2011
Available online 3 November 2011

Keywords:
Direct methanol fuel cell
Proton exchange membrane
Selectivity
Methanol crossover
Water diffusion

ABSTRACT

Selective sulfonated poly(imide)s with high proton conductivity and low methanol permeability were tested for their performance as proton exchange membranes in direct methanol fuel cells (DMFC). The proton to methanol transport selectivity of the poly(imide) membranes correlated well with the self-diffusion coefficients of water in the membranes as determined by pulsed-field gradient nuclear magnetic resonance. The poly(imide) membranes showed improved fuel cell device performance, however high interfacial resistance between the membranes and electrodes decreased the membrane electrode assembly (MEA) conductivity to methanol crossover selectivity, likely due to the use of NAFION®-based electrodes. The maximum power densities of SPI-50, SPI-75, and NR-212 based MEAs were 75, 72, and 67 mW cm^{-2}, respectively, with a methanol feed concentration of 2 M at a cell temperature of 60 °C.

1. Introduction

Fuel cells have been recognized as one of the next-generation power source technologies for future mobile and stationary applications [1,2]. The attractiveness of fuel cells lies in their high energy densities compared to batteries and capacitors due to their use of chemical fuels, such as methanol [3]. For portable applications, proton exchange membrane fuel cells (PEMFCs) have proven to be the most promising choice of fuel cell technology in terms of their low operation temperature, robust architecture, and rapid start-up/shut-down speeds. Most state-of-the art PEMFC devices are based on poly(perfluosulfonic acid) membranes, such as NAFION®, as this commercial platform provides high conductivity, good chemical stability, ease of processing for device fabrication, and reproducibility in large volumes.

A perceived weakness of NAFION® in portable DMFC applications is its high methanol permeability. Methanol diffusing from the anode to cathode in a methanol-fed cell can lower the cell output voltage due to a mixed potential at the cathode and decrease the fuel efficiency of the device. Engineering strategies have been developed to combat methanol crossover, such as operating the cell at the anode limiting current or incorporating methanol barriers at the anode side of the cell [4,5]. Both of these methods lower the effective methanol concentration on the anode side of the membrane and subsequently decrease the methanol crossover due to the decrease in methanol concentration gradient across the membrane. These approaches have brought DMFCs to the cusp of widespread commercialization, but they impose certain operational constraints on the system and limit the dynamic operating range of the cell. Proton exchange

* *Corresponding author*. Tel.: +1 814 867 1847; fax: +1 814 865 2917.
E-mail address: hickner@matse.psu.edu (M.A. Hickner).
0360-3199/$ – see front matter Copyright © 2011, Hydrogen Energy Publications, LLC. Published by Elsevier Ltd. All rights reserved.
doi:10.1016/j.ijhydene.2011.09.092

membranes (PEM) with intrinsically lower methanol permeability will enable a wider operating window for DMFCs and hold the possibility of increasing the efficiency of liquid-fed cells.

There has been considerable effort focused on developing new polymers for use as proton exchange membranes [6,7]. Many promising materials that have been demonstrated in operating cells are based on sulfonated aromatic polymer architectures such poly(sulfone)s, poly(ketone)s, poly(-phenylene)s, and poly(imide)s [8–16]. Generally, these types of polymers have yielded disappointing conductivity performance in hydrogen/air fuel cells at low relative humidity, but many sulfonated polymers with aromatic backbones have been shown to be suited to application in direct methanol fuel cells due to their low methanol crossover [17,18]. The electrochemical selectivity of PEMs, defined by the ratio of their proton conductivity to methanol permeability, has been used to gauge the potential of new materials to be used in DMFCs [19]. Several classes of high selectivity membranes have been reported and extremely high selectivity in novel membranes has been achieved [20,21], but these types of membranes generally have lower conductivity than desired, below 30 mS cm^{-1} in liquid water at 30 °C, for application in a device. Relative selectivities, the selectivity of the membrane divided by the selectivity of NAFION®, between 2 and 10 have been reported in membranes that have sufficient conductivity for operation in high current density devices [22–25]. These membranes have shown state-of-the-art DMFC performance, but the drastic increase in selectivity compared to NAFION® has not dramatically increased the performance of the cell.

High selectivity in PEMs is thought to stem from the interaction of absorbed water with the polymer backbone. Aromatic polymers are known to have smaller hydrophilic domains than NAFION® [26,27], and have more polarizable backbone moieties compared to NAFION®'s perfluorinated architecture. Kim et al. [28] correlated the calorimetric and NMR signatures of absorbed water in NAFION® and sulfonated poly(ether sulfone) with the membranes' conductivity, electro-osmotic drag, and methanol permeability. These authors observed that a greater fraction of water was strongly associated with the poly(ether sulfone) membrane compared to more bulk-like water behavior in NAFION®. Because the methanol, proton, and water transport in PEMs occurs within the hydrophilic phase, strategies to modify the character of the water-filled domain structure in fuel cell membranes often result in a trade-off between increasing proton conductivity, which promotes higher permeability and electro-osmotic drag, or decreasing methanol permeability which tends to decrease proton conductivity [29]. Higher conductivity is desired which is facilitated by having more bulk-like water in the membrane, but water that has lower association with the polymer backbone also tends to increase the methanol permeability of the material. When the water becomes more tightly bound within the polymer matrix, methanol permeability is suppressed, but often proton conductivity suffers as well. Designing highly selective PEMs requires optimizing the ion exchange capacity, water swelling, domain structure, and water interactions such that there is a high concentration and high connectivity of sulfonic acid groups to facilitate proton transport, while not having a large amount of loosely bound water, which drastically increases the methanol permeability.

Sulfonated poly(imide)s (SPIs) have been investigated as potential PEM materials by several groups [8,9,30]. SPIs have shown promising attributes in terms of their low methanol crossover and sufficient conductivity. However, most of the SPIs that have been reported are not stable in water at high temperature because of the hydrolysis of imide rings, even when considering 6-membered naphthalimides [31], which are much more stable than the 5-membered imides. Recently, we reported a series of sulfonated poly(imide)s based on 4,4′-binaphthyl-1,1′,8,8′-tetracarboxylic dianydride (BNTDA), Fig. 1 [32]. These BNTDA-based poly(imide)s showed excellent hydrolytic stability because of the unique linkage of two non-coplanar naphthalimide moieties by a single covalent bond, which is a different architecture than the electronically conjugated naphtalimide groups in 1,4,5,8-naphthalenetetracarboxylic dianhydride-based poly(imide)s. Separated naphthalimide rings have higher electron density in the carbonyl carbons, which decreases the likelihood of nucleophilic attack at this position and thus increases the membrane stability. In this paper, we report the transport properties of the BNTDA-based sulfonated poly(imide) membranes and the correlation between their selectivity and water self-diffusion coefficient. We then show that sulfonated poly(imide)s displayed robust performance in methanol and hydrogen-fed fuel cells.

2. Experimental

2.1. Membrane and MEA preparation

The BNTDA-based SPI membranes were synthesized and cast from solution according to the procedures reported in the literature [32]. The two types of SPI membranes studied in this work were SPI-50 and SPI-75, which contained 50 or 75 mol% of the sulfonated diamine, $x = 0.5$ or 0.75 in Fig. 1. After solution casting and drying, the membranes were boiled in 0.5 M H_2SO_4 for 5 h, washed thoroughly with deionized water, and stored in water for at least 24 h before characterization. NAFION® NR-212 was used as received from Ion Power, Inc. (New Castle, DE).

All MEAs with active area of 12 cm^2 employed NAFION® 1100 as the ionomer in the electrodes. The prepared ink was direct sprayed onto the membranes which were placed on a vacuum platform heated to 70 °C. The loadings of Pt/Ru black and Pt black in the anode and cathode catalyst layers were 6 and 4 mg cm^{-2}, respectively, with 1 mg cm^{-2} NAFION® loading in each electrode. Carbon paper GDLs were hot pressed onto the electrodes following Ref. [33].

2.2. Fuel cell characterization

The prepared MEAs were mounted between two identical graphite flow plates with two-path serpentine channels. Cell performance was evaluated at 60 °C with 2 M methanol at a flow rate of 0.19 mL min^{-1} (a stoichiometry of 2 at 150 mA cm^{-2}) fed to the anode and air at flow rates of 98, 163 and 326 mL min^{-1} (at stoichiometires of 3, 5 and 10 calculated at 150 mA cm^{-2}) fed to the cathode. An electronic load (BT4,

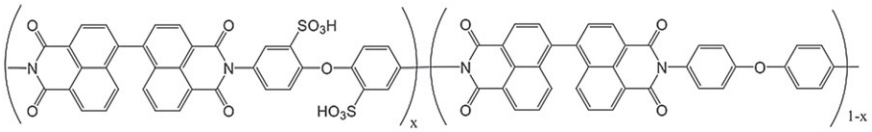

Fig. 1 – Chemical structure of BNTDA-based sulfonated poly(imide); $x = 0.75$ for SPI-75 and 0.5 for SPI-50.

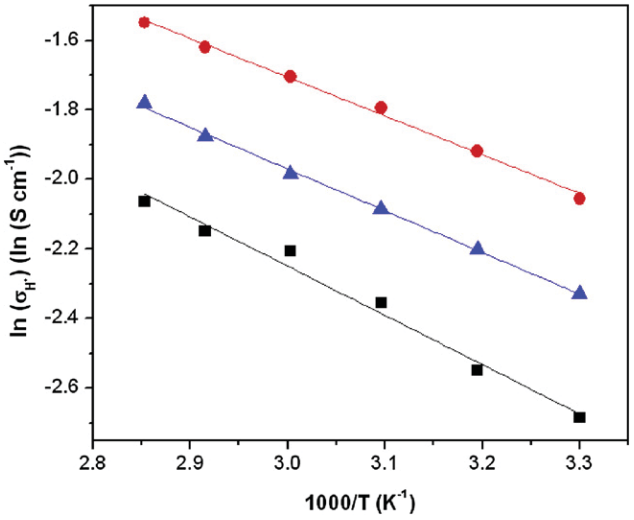

Fig. 2 – Arrhenius plot of conductivity for (●) SPI-75, (■) SPI-50, and (▲) NR-212 in liquid water.

Arbin Instruments, College Station, TX) in the galvanodynamic mode was used to measure the polarization curve at a scan rate of 3 mA s^{-1}. The steady-state performance of the cells was also measured with controlled current density of 150 mA cm^{-2}. During the test, a milliohm meter was used to measure the high frequency resistance (HFR) of the MEAs.

Anode limiting current [34] and H_2/air cathode polarization at a cell temperature of 60 °C were measured in order to evaluate individual electrode performance. For the anode limiting measurement, 2 M methanol with a flow rate of 0.19 mL min^{-1} was fed to the anode side, while H_2 with a flow rate of 100 mL min^{-1} was supplied at the cathode side of the cell to serve as a dynamic hydrogen reference electrode. In the cathode polarization measurement, 100% humidified H_2 at a flow rate of 100 mL min^{-1} was supplied into the anode side, while fully humidified air was fed to the cathode at a flow rate of 326 mL min^{-1}.

In order to evaluate the methanol crossover of the tested membrane in the MEAs [35], 2 M methanol was supplied to the anode side with a methanol flow rate of 2.5 mL min^{-1} with fully-humidified nitrogen fed to the cathode at a flow rate of 100 mL min^{-1}. At this high methanol feed rate, the limiting current density during cell polarization was independent of methanol flow rate. Thus, the effect of methanol consumption along the flow field could be ignored and the assumption of a uniform methanol concentration from inlet to outlet was valid.

2.3. *Membrane characterization*

The in-plane resistance of the membranes was measured by two-probe electrochemical impedance spectroscopy using a Solartron 1260A (Oak Ridge, TN) Impedance/Gain-Phase Analyzer. The impedance measurements were recorded with the membrane immersed in liquid water using a cell of similar design to that reported previously [36]. The activation energy for proton conduction, $E_{a,\sigma}$, was calculated from conductivity measurements between 30 and 70 °C (in 10 °C steps) assuming Arrhenius behavior.

Methanol permeability (P_{CH_3OH}) was measured using a membrane-separated concentration cell equipped with a refractive index detector for monitoring the change in methanol concentration versus time in the pure water compartment as described in the literature [37]. Methanol permeability was obtained at 30 and 70 °C (in 10 °C steps) and the activation energy, E_{a,CH_3OH}, was calculated in a similar fashion to the activation energy for proton conduction [26].

Pulsed-field gradient water self-diffusion measurements were obtained using a 5 mm broadband gradient probe on a Bruker (Billerica, MA) spectrometer using a stimulated echo sequence. The gradient was varied in 16 steps from 2% to 95%

Table 1 – Properties of BNTDA-based SPI and NR-212 membranes.

	IEC (meq g^{-1})[a]	wu (%)[b]	σ_{H^+} (mS cm^{-1})[c]	P_{CH_3OH} (cm^2 s^{-1})[d]	RS[d]	$E_{a,\sigma}$ (kJ mol^{-1})	E_{a,CH_3OH} (kJ mol^{-1})	D_{eff} (cm^2 s^{-1})[b]
SPI-75	2.21	53	182	1.4×10^{-6}	2.6	9.3	16.2	7.6×10^{-6}
SPI-50	1.57	38	110	6.1×10^{-7}	3.5	11.8	25.2	2.0×10^{-7}
NR-212	0.91	36	137	2.7×10^{-6}	1	10.0	18.3	9.5×10^{-6}

a From NMR.
b Fully hydrated 30 °C.
c 60 °C in liquid water.
d 60 °C.

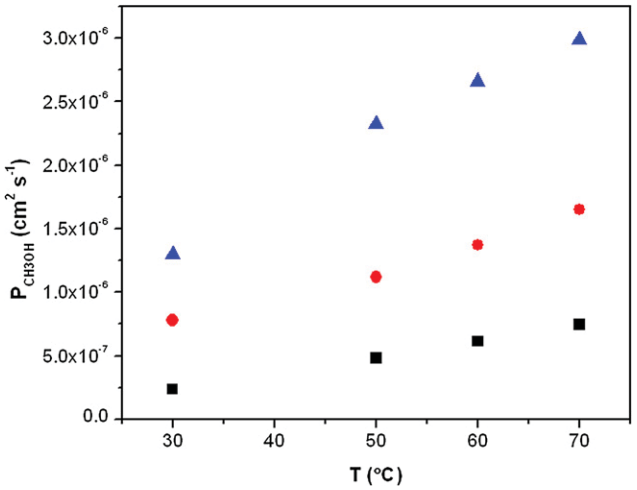

Fig. 3 – Methanol permeability of (●) SPI-75, (■) SPI-50, and (▲) NR-212 as a function of temperature.

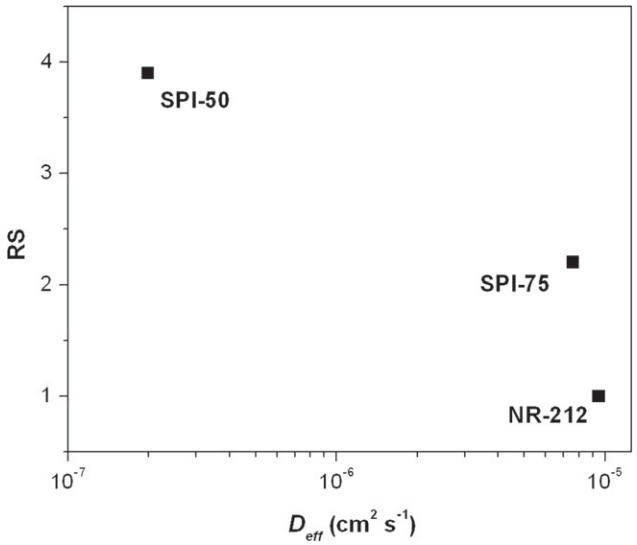

Fig. 5 – Relative selectivity (RS) versus water self-diffusion coefficient (D_{eff}) for the membranes in this study at 30 °C.

of the maximum gradient strength, 71.9 G cm^{-1}. The decay of the signal density, I, is given by:

$$I - I_0 \exp\left[- D_{eff}(G\delta\gamma)^2(\Delta - \delta/3)\right] \quad (1)$$

where I_0 is the initial signal density, D_{eff} is the effective diffusion coefficient (m^2 s^{-1}), G is the gradient strength, δ is the length of the gradient length, γ is the gyromagnetic ratio of the observed nuclei, and Δ is the diffusion time. In these experiments, Δ is 90 ms, δ is 1 ms, and γ is 2.68 × 10^8 rad s^{-1} T^{-1}. The natural log of I/I_0 versus $(G\delta\gamma)^2(\Delta - \delta/3)$ was linearly regressed and the negative of the slope was taken as the effective diffusion coefficient.

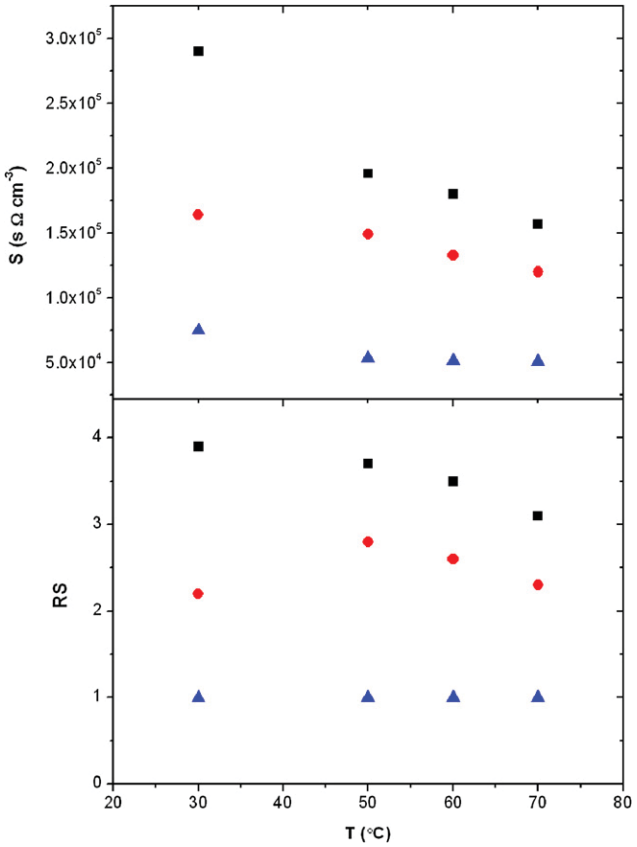

Fig. 4 – Selectivity (S), top, and relative selectivity (RS), bottom, for (▲) NR-212, (●) SPI-75, and (■) SPI-50.

3. Results and discussion

The proton conductivity (σ_{H^+}) of the membranes was measured during immersion of the membranes in liquid water at different temperatures. The natural logarithm of the conductivity was plotted against inverse temperature in an Arrhenius fashion as shown in Fig. 2 and the activation energies of proton conduction ($E_{a,\sigma}$) were calculated and listed

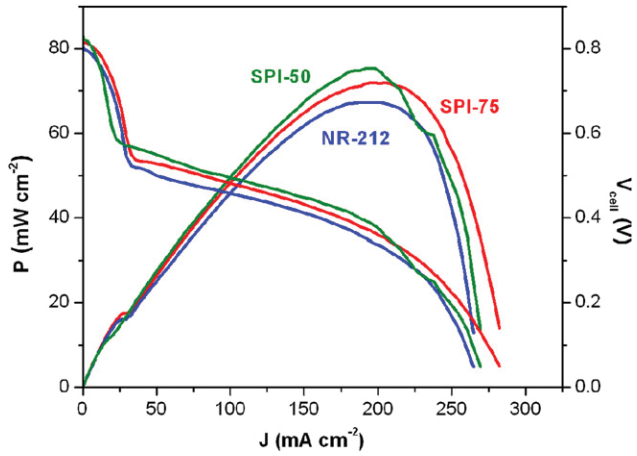

Fig. 6 – DMFC polarization and power density curves for NR-212 (60 μm), SPI-75 (30 μm), and SPI-50 (20 μm)-based MEAs; 2 M CH_3OH, 60 °C, SR_a/SR_c = 2/5.

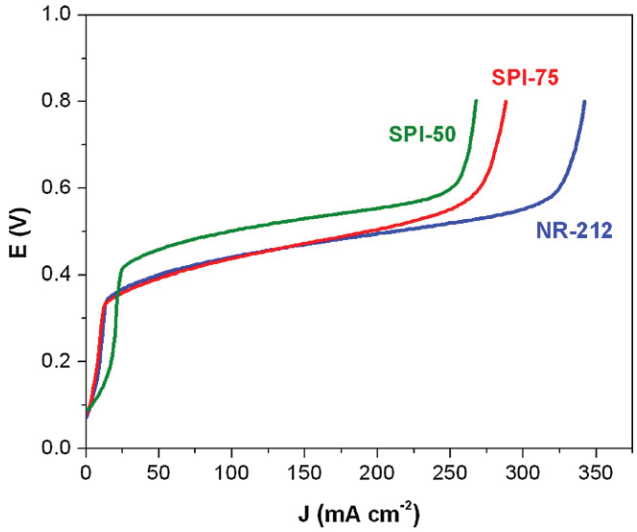

Fig. 7 – Limiting CH_3OH crossover current density of NAFION® and SPI-based MEAs; 2 M CH_3OH, 2.5 mL min^{-1} anode flow rate, T_{cell} = 60 °C.

in Table 1. The activation energies of the samples followed a trend of SPI-50 > NR-212 > SPI-75 which was inverse of the trend observed for the magnitudes of the proton conductivity.

NR-212 displayed the highest methanol permeability of the samples, Fig. 3, which is interesting considering that it had the lowest bulk water uptake. The low activation energies calculated for methanol permeation in NR-212 and SPI-75, Table 1, indicate that the diffusion of methanol is facile in these materials, but SPI-75 has 50% higher bulk water uptake (wu) than NR-212. SPI-50 has similar bulk water uptake to NR-212, yet it had a much higher E_{a,CH_3OH} and four times lower methanol permeability. As methanol transport occurs through the water-filled domains in PEMs, it is clear that the absorbed water in each of these membranes has different characteristics.

Given the temperature-dependent data for conductivity and methanol permeability, the selectivity (S) of SPI membranes was computed for the range of temperatures of interest in this study, Fig. 4. The selectivity declined with temperature for the two SPI membranes above 50 °C, but was relatively constant for NR-212 between 50 and 70 °C. The relative selectivity (RS) of the two SPI membranes remained greater than unity across the temperature range of interest. It is thought that the origin of low methanol permeability and high selectivity in sulfonated poly(aromatic) membranes, like the sulfonated poly(imide)s studied in this work, is due to the smaller characteristic length scale of their hydrophilic domain morphology compared to NAFION® [26,27]. This difference in morphology is often manifest in the diffusion properties of water within the hydrophilic network. The effective water self-diffusion coefficients (D_{eff}) of the SPI membranes and NR-212 were measured via PFG-NMR, and the values correlated strongly with the observed relative selectivities, Fig. 5. This correlation indicates that water motion in these membranes is critical to determining their transport properties and the balance between proton conductivity and methanol permeability.

Table 2 – Properties of NAFION® and SPI-based MEAs.

	t (μm)	HFR (Ω cm^2)[a]	I_{lim} (mA cm^{-2})[b]	RS_{MEA}[b]	OCV_{CH_3OH} (V)[a]	P_{max,CH_3OH} (mW cm^{-2})[a]	OCV_{H_2} (V)[c]	P_{max,H_2} (mW cm^{-2})[c]
SPI-75	30	0.103	288	1.0	0.82	72	0.95	252
SPI-50	20	0.097	267	1.1	0.83	75	0.95	250
NR-212	60	0.083	342	1.0	0.80	67	0.95	238

a Methanol concentration of 2 mol/L, SR_a/SR_c = 2/5, T = 60 °C.
b 60 °C.
c 100% humidified H_2 at a flow rate of 100 mL min^{-1}, 100% humidified air at a flow rate of 326 mL min^{-1}, T = 60 °C.

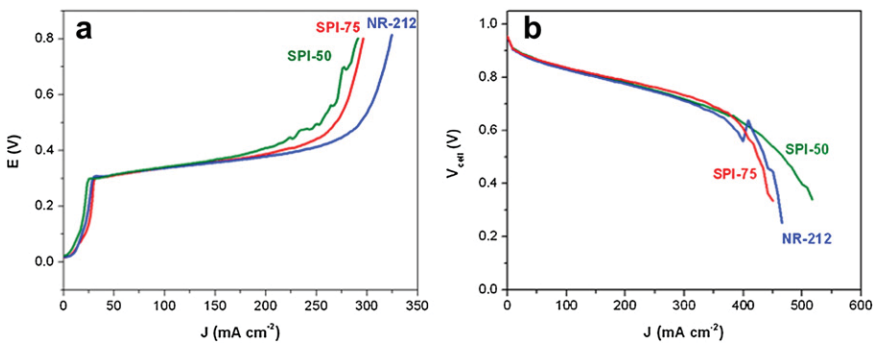

Fig. 8 – (a) Anode polarization (2 M CH_3OH, SR_a = 2 @ 150 mA cm^{-2}, T_{cell} = 60 °C) and (b) H_2/air polarization (100% humidified gases, anode flow rate = 100 mL min^{-1}, cathode flow rate = 326 mL min^{-1}, T_{cell} = 60 °C) of NAFION® and SPI-based MEAs.

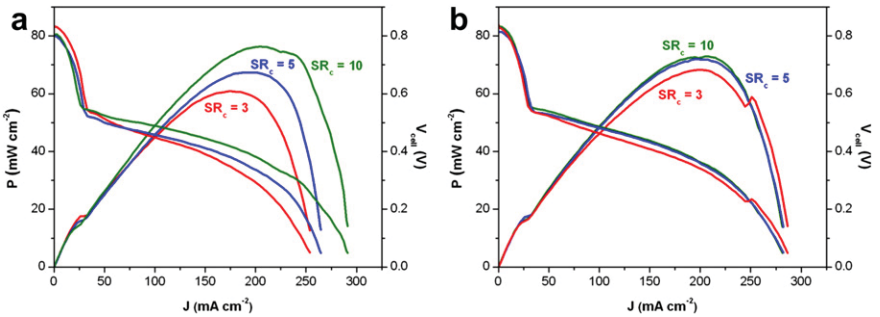

Fig. 9 – DMFC polarization and power density curves of NR-212 and SPI-75-based MEAs with different air stoichiometries; (a) NR 212, Red: SR_a/SR_c = 2/3, HFR = 0.081 Ω cm^2, Blue: SR_a/SR_c = 2/5, HFR = 0.083 Ω cm^2, Green: SR_a/SR_c = 2/10, HFR = 0.085 Ω cm^2; (b) SPI-75, Red: SR_a/SR_c = 2/3, HFR = 0.093 Ω cm^2, Blue: SR_a/SR_c = 2/5, HFR = 0.103 Ω cm^2, Green: SR_a/SR_c = 2/10, HFR = 0.119 Ω cm^2. ('For interpretation of the references to colour in this figure legend, the reader is referred to the web version of this article'.)

Considering their lower methanol permeability, thinner SPI membranes (30 μm for SPI-75, and 20 μm for SPI-50) can be used for DMFC applications without greatly increasing the flux of methanol to the cathode. The high frequency resistance (HFR) measured for MEAs at 60 °C was 0.083 (NR-212), 0.103 (SPI-75), and 0.097 (SPI-50) Ω cm^2 and a comparison of DMFC performance for these three samples is shown in Fig. 6. Although the projected in-cell membrane resistance of the SPIs is lower than that of NR-212 (based on the membrane thickness and conductivity), the measured HFRs were higher, likely due to membrane-electrode interfacial resistances in the SPI-based MEAs. It has been shown previously that highly swollen membranes can have greater interfacial resistances [38], therefore, even though SPI-75 is more conductive than SPI-50, the SPI membrane with the higher water uptake gave a higher HFR in MEA tests.

The NR-212-based MEA had a slightly lower OCV than the SPI membrane-based MEAs, which was a result of the higher methanol crossover of NR-212 relative to the SPI membranes. The power outputs of the MEAs based on SPI membranes were higher than the power production of the cell with the NR-212 MEA. The maximum power density (P_{max,CH_3OH}) of the SPI-50 MEA was 76 mW cm^{-2}, which was 11% higher than that of the NR-212 MEA (65 mW cm^{-2}). As the HRF of the SPI MEAs was higher than that of the NR-212 MEA, the low methanol crossover in the SPI membrane-based cells was the primary factor in their higher DMFC performance. Methanol crossover to the cathode leads to a mixed potential by oxidation of methanol on the cathode catalyst thus impeding oxygen reduction. Methanol oxidation at the cathode also consumes oxygen and generates excess water on the cathode side of the cell. SPI membranes have the advantage of lower methanol permeability based on both *in-situ* and *ex-situ* measurements, which is the key benefit of using this new type of membrane for DMFC applications. Another possible advantage of SPI-based membranes is their lower water transport properties as measured by D_{eff}. NR-212-based MEAs in DMFCs can suffer from cathode flooding at low cathode stoichiometries which reduces oxygen transport to the reaction sites and decreases the effective catalyst area. Based on the effective water self-diffusion coefficients, water transport in SPI membranes is lower than in NR-212, which could reduce cathode flooding and may increase the fuel cell performance when the cathode flow rates are low.

The methanol crossover of NR-212 and SPI-based MEAs was evaluated by measuring the limiting crossover current density at open circuit, Fig. 7. According to the limiting current density data, the methanol crossover of SPI-based MEAs was 15% (SPI-75) and 22% (SPI-50) lower than that of NR-212-based MEA. The relative selectivity of the MEAs (RS_{MEA}) was calculated from the HFR and methanol crossover limiting current measurements. The data in Table 2 show that the MEA selectivity for all three samples was near unity and is an indication for why all of the MEAs showed similar performance in a device. The MEA selectivity was much lower than the membrane selectivity (Table 1). The similarities in DMFC performance can be attributed directly to the membranes as the anode and cathode electrodes had similar polarization characteristics for all cells. The methanol oxidation capacity of the anodes and cathode polarization of each MEA were measured, Fig. 8. The NR-212 and SPI-based MEAs had similar anode and cathode kinetics for methanol oxidation and oxygen reduction.

The power production of NR-212 and SPI-75 based MEAs was compared over a range of cathode stoichiometries, Fig. 9. At low cathode stoichiometry, 3 and 5, SPI-75 based MEA showed better performance due to its lower methanol crossover. At a high cathode flow rate (stoichiometry 10), NR-212-based MEA showed better performance. Increasing the stoichiometry effectively increases the oxygen concentration at the cathode, thus methanol crossover can be combated, to a point, with increased cathode flow rate. Additionally, the low water transport in SPI-75 could be a detriment at high stoichiometry due to cathode dry out, which is indicated by an HFR increase from 0.093 to 0.119 Ω cm^2 when the cathode stoichiometry was increased from 3 to 10. Meanwhile, a higher air flow rate could decrease cathode flooding for the NR-212 MEA.

4. Conclusions

The proton conductivity and methanol permeability of sulfonated poly(imide) membranes and NAFION® NR-212

were compared at different temperatures and the activation energies for transport were calculated assuming Arrhenius behavior. The proton conductivity followed the trend of SPI-50 < NR-212 < SPI-75, and the methanol permeability of the both of the SPI membranes were less than that of NR-212. Based on the PFG-NMR results, the water in SPI membranes showed much lower water self-diffusion coefficients, which were correlated to the proton conductivity to methanol permeability selectivity of the membranes. SPI-based MEAs showed higher maximum power densities in both direct methanol and hydrogen fuel cells, in spite of their greater high frequency resistance, which could be attributed to the lower methanol crossover and the decrease of cathode flooding due to the SPI membranes' low water permeability.

Acknowledgements

Partial support for this work was provided by NSF grant # CBET-0932740.

REFERENCES

[1] Jacobson MZ, Colella WG, Golden DM. Cleaning the air and improving health with hydrogen fuel-cell vehicles. Science 2005;308:1901–5.
[2] Steele BCH, Heinzel A. Materials for fuel-cell technologies. Nature 2001;414:345–52.
[3] Zelenay P, Piela P. Researchers redefine the dmfc roadmap. The Fuel Cell Review 2004;1:17–23.
[4] Liu FQ, Lu GQ, Wang CY. Low crossover of methanol and water through thin membranes in direct methanol fuel cells. Journal of the Electrochemical Society 2006;153:A543–53.
[5] Stanis RJ, Lambert TN, Yaklin MA. Poly(3,4-ethylenedioxythiphene) (pedot)-modified anodes: reduced methanol crossover in direct methanol fuel cells. Energy & Fuels 2010;24:3125–9.
[6] Hickner MA, Ghassemi H, Kim YS, Einsla BR, McGrath JE. Alternative polymer systems for proton exchange membranes (PEMs). Chemical Reviews 2004;104:4587–611.
[7] Jones DJ, Roziere J. Advances in the development of inorganic-organic membranes for fuel cell applications. Fuel Cells 2008;215:219–64.
[8] Fang JH, Guo XX, Harada S, Watari T, Tanaka K, Kita H, et al. Novel sulfonated polyimides as polyelectrolytes for fuel cell application. 1. synthesis, proton conductivity, and water stability of polyimides from 4,4'-diaminodiphenyl ether-2,2'-disulfonic acid. Macromolecules 2002;35:9022–8.
[9] Genies C, Mercier R, Sillion B, Cornet N, Gebel G, Pineri M. Soluble sulfonated naphthalenic polyimides as materials for proton exchange membranes. Polymer 2001;42:359–73.
[10] Ghassemi H, McGrath JE. Synthesis and properties of new sulfonated poly(p-phenylene) derivatives for proton exchange membranes. I. Polymer 2004;45:5847–54.
[11] Li XF, Liu CP, Lu H, Zhao CJ, Wang Z, Xing W, et al. Preparation and characterization of sulfonated poly(ether ether ketone ketone) proton exchange membranes for fuel cell application. Journal of Membrane Science 2005;255:149–55.
[12] Miyatake K, Chikashige Y, Higuchi E, Watanabe M. Tuned polymer electrolyte membranes based on aromatic polyethers for fuel cell applications. Journal of the American Chemical Society 2007;129:3879–87.
[13] Poppe D, Frey H, Kreuer KD, Heinzel A, Mulhaupt R. Carboxylated and sulfonated poly(arylene-co-arylene sulfone)s: thermostable polyelectrolytes for fuel cell applications. Macromolecules 2002;35:7936–41.
[14] Wang F, Hickner M, Kim YS, Zawodzinski TA, McGrath JE. Direct polymerization of sulfonated poly(arylene ether sulfone) random (statistical) copolymers: candidates for new proton exchange membranes. Journal of Membrane Science 2002;197:231–42.
[15] Wu SQ, Qiu ZM, Zhang SB, Yang XR, Yang F, Li ZY. The direct synthesis of wholly aromatic poly(p-phenylene)s bearing sulfobenzoyl side groups as proton exchange membranes. Polymer 2006;47:6993–7000.
[16] Xing PX, Robertson GP, Guiver MD, Mikhailenko SD, Kaliaguine S. Sulfonated poly(aryl ether ketone)s containing the hexafluoroisopropylidene diphenyl moiety prepared by direct copolymerization, as proton exchange membranes for fuel cell application. Macromolecules 2004;37:7960–7.
[17] Deluca NW, Elabd YA. Polymer electrolyte membranes for the direct methanol fuel cell: a review. Journal of Polymer Science Part B-Polymer Physics 2006;44:2201–25.
[18] Neburchilov V, Martin J, Wang HJ, Zhang JJ. A review of polymer electrolyte membranes for direct methanol fuel cells. Journal of Power Sources 2007;169:221–38.
[19] Pivovar BS, Wang YX, Cussler EL. Pervaporation membranes in direct methanol fuel cells. Journal of Membrane Science 1999;154:155–62.
[20] Siu A, Pivovar B, Horsfall J, Lovell KV, Holdcroft S. Dependence of methanol permeability on the nature of water and the morphology of graft copolymer proton exchange membranes. Journal of Polymer Science Part B-Polymer Physics 2006;44:2240–52.
[21] Xu K, Li K, Ewing CS, Hickner MA, Wang Q. Synthesis of proton conductive polymers with high electrochemical selectivity. Macromolecules 2010;43:1692–4.
[22] Kim DS, Kim YS, Guiver MD, Pivovar BS. High performance nitrile copolymers for polymer electrolyte membrane fuel cells. Journal of Membrane Science 2008;321:199–208.
[23] Lin J, Wu PH, Wycisk R, Trivisonno A, Pintauro PN. Direct methanol fuel cell operation with pre-stretched recast Nafion®. Journal of Power Sources 2008;183:491–7.
[24] Liu B, Hu W, Robertson GP, Kim YS, Jiang Z, Guiver MD. Sulphonated biphenylated poly(aryl ether ketone)s for fuel cell applications. Fuel Cells 2010;10:45–53.
[25] Sankir M, Kim YS, Pivovar BS, McGrath JE. Proton exchange membrane for dmfc and H_2/air fuel cells: synthesis and characterization of partially fluorinated disulfonated poly(arylene ether benzonitrile) copolymers. Journal of Membrane Science 2007;299:8–18.
[26] Hickner MA, Fujimoto CH, Cornelius CJ. Transport in sulfonated poly(phenylene)s: proton conductivity, permeability, and the state of water. Polymer 2006;47:4238–44.
[27] Kreuer KD. On the development of proton conducting polymer membranes for hydrogen and methanol fuel cells. Journal of Membrane Science 2001;185:29–39.
[28] Kim YS, Dong LM, Hickner MA, Glass TE, Webb V, McGrath JE. State of water in disulfonated poly(arylene ether sulfone) copolymers and a perfluorosulfonic acid copolymer (Nafion) and its effect on physical and electrochemical properties. Macromolecules 2003;36:6281–5.
[29] Hickner MA, Pivovar BS. The chemical and structural nature of proton exchange membrane fuel cell properties. Fuel Cells 2005;5:213–29.
[30] Asano N, Aoki M, Suzuki S, Miyatake K, Uchida H, Watanabe M. Aliphatic/aromatic polyimide lonomers as

a proton conductive membrane for fuel cell applications. Journal of the American Chemical Society 2006;128: 1762–9.
[31] Einsla BR, Kim YS, Hickner MA, Hong YT, Hill ML, Pivovar BS, et al. Sulfonated naphthalene dianhydride based polyimide copolymers for proton-exchange-membrane fuel cells II. membrane properties and fuel cell performance. Journal of Membrane Science 2005;255: 141–8.
[32] Yan JL, Liu CP, Wang Z, Xing W, Ding MM. Water resistant sulfonated polyimides based on 4,4'-binaphthyl-1,1',8,8'-tetracarboxylic dianhydride (BNTDA) for proton exchange membranes. Polymer 2007;48:6210–4.
[33] Lim C, Wang CY. Development of high-power electrodes for a liquid-feed direct methanol fuel cell. Journal of Power Sources 2003;113:145–50.
[34] Ren X, Springer TE, Gottesfeld S. Water and methanol uptakes in Nafion membranes and membrane effects on direct methanol cell performance. Journal of the Electrochemical Society 2000;147:92–8.
[35] Ren XM, Springer TE, Zawodzinski TA, Gottesfeld S. Methanol transport through Nafion membranes - electro-osmotic drag effects on potential step measurements. Journal of the Electrochemical Society 2000;147:466–74.
[36] Fujimoto CH, Hickner MA, Cornelius CJ, Loy DA. Ionomeric poly(phenylene) prepared by diels-alder polymerization: synthesis and physical properties of a novel polyelectrolyte. Macromolecules 2005;38:5010–6.
[37] Kim YS, Hickner MA, Dong LM, Pivovar BS, McGrath JE. Sulfonated poly(arylene ether sulfone) copolymer proton exchange membranes: composition and morphology effects on the methanol permeability. Journal of Membrane Science 2004;243:317–26.
[38] Pivovar BS, Kim YS. The membrane-electrode interface in PEFCs. Journal of the Electrochemical Society 2007;154: B739–44.